I&EC research
Industrial & Engineering Chemistry Research

Article

pubs.acs.org/IECR

Biopolymer-Based Nanofiber Mats and Their Mechanical Characterization

Shahrzad Khansari,[†] Suman Sinha-Ray,[†] Alexander L. Yarin,*[,†,‡] and Behnam Pourdeyhimi[§]

[†]Department of Mechanical and Industrial Engineering, University of Illinois at Chicago, 842 W. Taylor St., Chicago, Illinois 60607-7022, United States

[‡]College of Engineering, Korea University, Seoul 136-701, South Korea

[§]3427 The Nonwovens Institute, North Carolina State University, Box 8301, Raleigh, North Carolina 27695-8301, United States

ABSTRACT: Nanofibers produced from plant- and animal-derived proteins using the solution-blowing method were collected and their mechanical properties were characterized and compared with those of synthetic polymer samples that were produced and collected similarly. Soy protein, zein, lignin, and cellulose acetate were the plant-derived proteins and silk protein (sericin) and bovine serum albumin were the animal-derived proteins used in the present work to form nanofibers by solution blowing. The aim of this work is to demonstrate that solution blowing can be successfully used to form nanotextured nonwovens from a number of biopolymers, which is of significant interest for a wide range of applications such as filtration, packaging, bioplastics and biomedical materials. Tensile tests were used to elucidate mechanical properties of such nanofiber mats. It was also shown that hot and cold drawing can be applied as a post-treatment to further enhance their mechanical performance.

1. INTRODUCTION

Due to the technological, environmental and political considerations, substituting traditional synthetic composites and plastics made of glass, polyesters, and other polymers by biodegradable natural biopolymers attracted significant attention since the 1990s. Such synthetic materials as reinforcers and fillers made of epoxy, polyurethanes, and phenolics remain stable after their usage period ends, which results in severe littering, environmental problems, and recycling concerns.[1,2] For example, biodegradation of blown poly(ethylene terephthalate) bottles revealed that 50% of material loss occurs in 30−40 years at 20 °C and 45−100% relative humidity.[3,4] It was also mentioned that film tapes take as long as 100 years for degradation in an environment under the above-mentioned conditions. The demand to replace synthetic products by sustainable and biodegradable materials stimulated research work on high-value biopolymer-derived materials that have mechanical properties comparable to those of the petroleum-derived ones. Humidity resistance, processability, and manufacturing costs are major issues for biodegradable materials that are produced from plant proteins (e.g., soy protein, starch, cellulose, lignin, and zein).[5−7]

Soy protein is one of the lowest cost and most abundant biopolymers[7,8] that is commercially used in plastics, fillers, and adhesives. Compression molding and extrusion are usually employed to produce soy plastics.[9−12] The United States is the largest producer of soy and soy protein isolates, with the latter often obtained as a byproduct of soy-derived biodiesel.

Cellulose is a natural polymer that had been isolated from plant structures over 150 years ago.[13] Cellulose has a fibrous structure and comprises a significant percentage of the wood parts in plant structures. In particular, over 40% of wood and 90% of cotton fiber structures are comprised of cellulose,[14−16] which makes wood pulp and cotton major commercial sources of the industrially available cellulose. Correspondingly, cellulose is commercially utilized in paper and textile industry. The protein structure of cellulose is heterogeneous and biocompatible and it holds great promise for biomedical and pharmaceutical applications.[13,17,18] Cellulose had been traditionally used as a source of biofuel,[19−21] albeit the current tendency is to find alternative high-value applications for it. Modern adhesives and liquid filtration industries are benefitting from cellulose utilization.[22−24] A considerable number of hydroxyl groups in the cellulose structure results in formation of hydrogen bonds in its macromolecule.[1,13,25] Therefore, the cellulose structure becomes aggregated. The intra- and interconnected network-like structure of cellulose is responsible for its insolubility in water and most of the organic solvents. Consequently, cellulose-containing materials (e.g., wood) possess noticeable strength associated with the aggregation and hydrogen bonds in their structure. Cellulose's insolubility in many solvents motivated the search for alternatives that possess cellulosic structure and properties but are relatively easily soluble in acidic and basic solutions. For example, acetate and nitrate esters are among the most widely used derivatives of cellulose, which are used as such alternatives. Cellulose acetate is thermally stable and nontoxic. These properties, as well as its solubility in common solvents, resulted in many applications of cellulose acetate. Cellulose acetate is used in adhesives, thermoplastics, coatings, and the textile industry.[24,26−30]

Lignin is an aromatic polymer that is found in cell walls of plants. It is responsible for their strength.[31] Lignin also protects plants from microbial infections.[31] It is a stable macromolecule and protects plants from degradation due to environmental conditions such as humidity and temperature. Typically, it is

Received: July 14, 2013
Revised: September 22, 2013
Accepted: October 2, 2013
Published: October 2, 2013

dx.doi.org/10.1021/ie402246x | *Ind. Eng. Chem. Res.* 2013, 52, 15104−15113

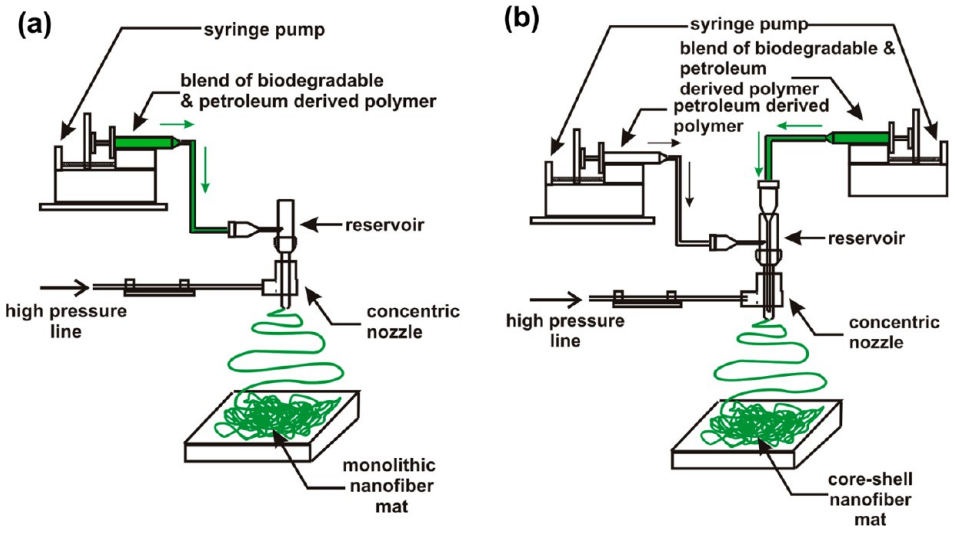

Figure 1. Sketch of the setup for solution blowing of monolithic nanofibers (a), and coblowing of core−shell nanofibers (b).

found in secondary cell walls of plants where lignin wraps cellulose microfibrils. On the other hand, primary cell walls are formed of cellulose.[32] Lignin is considered to be the second most abundant natural biopolymer; cellulose is the most abundant. Lignin, similarly to cellulose, had traditionally been used as a source for biofuel, albeit the current tendency is to find alternative applications for this plant-derived biopolymer. Lignin macromolecules possess a variety of different structures, being either sulfur-containing or sulfur-free. The complex aromatic structure of lignin, which also contains both hydrophilic and hydrophobic groups, is cross-linked and aggregated, which results in significant strength in this material. Lignin is used in cosmetic and antibacterial materials, adhesives, and surfactants.[33] Lignin is a major byproduct of the paper industry, and as such is abundant, which fuels research on its novel applications, in particular as a precursor to carbon fibers.[33−35] Lightweight and strong carbonaceous materials find applications in the aerospace and aviation industries.[36,37]

Zein constitutes up to 50% of protein in corn structure. It has been isolated from corn in the early 19th century. Corn structure consists of endosperm, which incorporates all zein.[38] Except as a human food, corn is used to extract starch and oil, as well as more recently to produce ethanol as a fuel.[38] According to refs 39 and 40, the major amino acid components in zein are proline, luecine, and alanine, which are hydrophobic. It is emphasized that zein does not contain a majority of essential amino acids; therefore, its value as a nutritional protein is quite restricted. Significant attention was paid to development of commercially available industrial polymers from zein. Some efforts were directed at forming nanofibers by electrospinning from a zein solution.[41−43]

Silk sericin is the major constituent of silk. Sericin is extracted from silk for different applications, such as pharmaceuticals and cosmetics.[44,45] It is functionalized to use in contact lenses and damaged tissues. It has noticeable adhesive properties and acts as a glue bonding fibroin together in the cocoon structure of silk. Sericin is blended with synthetic polymers and resins to acquire materials with comparable properties with those of synthetic ones. Electrospinning of *Bombyx mori* silk with poly(ethylene oxide) was reported in refs 46 and 47. When sericin is dumped as waste in water, it acts as a pollutant, increasing biological and chemical oxygen demand. On the other hand, sericin can also be used as a very useful biomaterial.[48]

The properties and structure of bovine serum albumin (BSA) are similar to those of serum albumin protein in human body. Therefore, BSA can be used as a characteristic protein to mimic human protein environment. Therefore, BSA nanofibers attracted significant attention in relation with wound dressing, cell growth, and drug carriers.[49,50] Core−shell electrospun nanofibers were formed with BSA in the core and polycaprolactone (PCL) in the shell.[51] The shell also contained PEG as a porogen. These nanofibers were used for controlled drug release. BSA fibers were functionalized as a biosensor.[52] Nerve growth factor (NGF) was released from BSA-PCL nanofibers.[53] The solubility of BSA in aqueous medium leads to the formation of pores in the nanofibrous structure, which finally results in NGF release from the fibrous carrier.

Although such plant- and animal-derived polymers as soy protein, starch, lignin, zein, sericin, and BSA have been extensively used in composites, fillers, coatings, and adhesives, their low cost, abundance, and specific protein structures hold great promise for their further utilization. Prior efforts to use these biopolymers as substitutes for synthetic materials were hindered by their relatively low strength and low water resistance as well as odor and color.

Formation of nanofibers from biologically derived proteins is limited to laboratory scale only due to the low throughput of electrospinning. In addition, the need for high voltage forces the industry to avoid electrospinning. In general, electrospinning of biologically derived polymers often results in spraying and low quality fibers. The present work aims at an en masse formation of nanofibers from animal and agricultural proteins using solution blowing. This method is much faster than electrospinning and does not depend on the electric properties of polymer solutions as the latter does. Solution blowing was recently introduced and applied to form soy protein nanofibers with rates 20−30 times faster than conventional electrospinning.[54,55] The solution-blowing method was also used in the work where monolithic and core−shell cellulose micro/nanofibers were produced.[56]

In the present work, solution blowing is applied to form nanofibers from soy protein, cellulose acetate, lignin, zein, sericin, and bovine serum albumin, and it also aims at their

dx.doi.org/10.1021/ie402246x | *Ind. Eng. Chem. Res.* 2013, 52, 15104−15113

mechanical characterization as an extension of our previous work.[57] In our previous works,[55,57,58] we demonstrated the possibility of preparing soy protein- and nylon-based nanofibers. In the present work, we have also demonstrated the possibility of preparing PET-based soy protein nanofibers. PET was chosen as the carrier polymer because it is a rigid and lightweight but strong polymer that does not swell in water like nylon. PET is used in cardiovascular surgery for blood vessels and artificial heart implantation[59−61] due to its noticeable mechanical properties and acceptable biocompatibility in the human body. As discussed in ref 62, artificial heart valves produced with PET are supposedly functional for up to 10 years in the body. This shows the possibility of using PET-containing nanofibers in biomedical applications.

In addition, in the present work post-processing is also applied to biodegradable solution-blown nanofibers to enhance their overall mechanical properties.

2. EXPERIMENT

2.1. Materials. Cellulose acetate (M_w = 30 KDa), zein, low sulfonate lignin alkali powder (M_w = 10 KDa), anhydrous *N*,*N*-dimethylformamide (99.8%), formic acid (grade >95%), anhydrous dichloromethane, DCM (≥99.8%), trifluoroacetic acid (TFA, ReagentPlus 99%), dichloroacetic acid (DCA, ReagentPlus ≥99%), Butvar B-98, and methanol (≥99.8%, A.C.S. reagent) were purchased from Sigma-Aldrich. Polyamide-6 (nylon-6) (M_w = 65.2 KDa) was provided by BASF. Polyacrylonitrile, PAN, (M_w = 150 KDa) and polyvinyl alcohol, PVA (M_w = 78 KDa) were purchased from PolySciences. Soy protein isolate [PRO-FAM 781 (SP 781)] was provided by ADM Specialty Food Ingredients. Granular poly(ethylene terephthalate), PET, was provided by NC State University. Silk sericin was obtained from Chagnsha Guanxiang Chemical Trading. Finally, bovine serum albumin−Cohn fraction V, protease-free, (BSA) was purchased from LEE Biosolutions. All materials were used without applying any post-treatment.

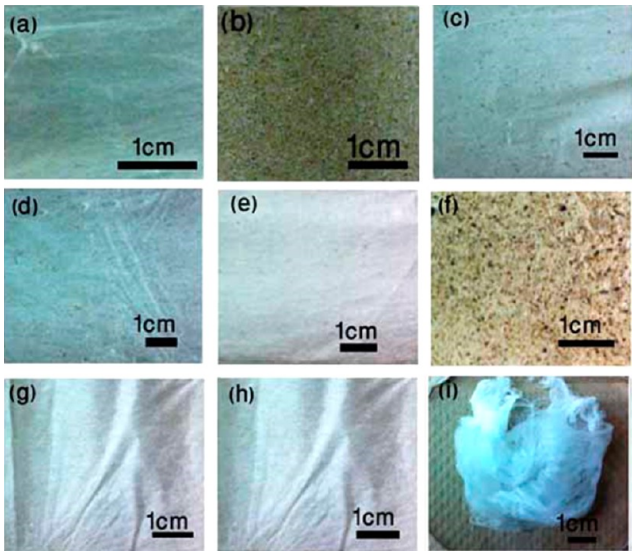

Figure 2. Panel a: Solution-blown cellulose acetate/PAN (50/50 wt %) nanofiber mat. Panel b: Soy protein/PET (20/80 wt %) nanofiber mat. Panel c: Soy protein/zein/nylon 6(25/25/50 wt %) nanofiber mat. Panel d: Zein/nylon 6 (57/43 wt %) nanofiber mat. Nanofiber mats in panels a−d are comprised of monolithic nanofibers. Panel e: Core−shell zein/nylon 6 nanofiber sample. Panel f: Monolithic lignin/nylon 6 (50/50 wt %) sample. Panel g: Monolithic zein/silk sericin/nylon 6 (25/25/50 wt %) nanofibers. Panel h: Monolithic silk sericin/nylon 6 (50/50 wt %). Panel i: Monolithic BSA/PVA (50/50 wt %) nanofiber sample.

2.2. Solution Preparation. A cellulose acetate/PAN solution was prepared by mixing 0.5 g of PAN in 9.5 g of DMF. The solution was left on a hot plate for 5 h at 60 °C. Then, 0.5 g of cellulose acetate was added to the PAN solution and stirred at room temperature for another hour.

Zein solution was prepared in three different contents. In separate vials, 1.0, 2.0, and 3.0 g of zein was mixed with 10.0 g of formic acid and left on a hot plate at 75 °C for 3 h. Then, 1.5 g of nylon 6 was added to each solution and left stirring on the hot plate at the same temperature for 24 h. To produce core−shell zein/nylon 6 nanofibers, solutions were prepared as follows. The core solution consisted of 3.0 g of zein that was mixed with 13 g of formic acid and left on a hot plate at 75 °C for 3 h. Next, 1.25 g of nylon 6 was added to the core solution and stirred on the hot plate for another day to make it homogeneous. The shell solution was 20 wt % nylon 6 in formic acid.

Soy protein/zein/nylon 6 solution was prepared by adding 0.75 g of SP 781 and 0.75 g of zein to 10 g of formic acid and leaving the solution on a hot plate at 80 °C for 12 h. After that, 1.5 g of nylon 6 was added, and the solution was left on a hot plate at 80 °C for stirring for 12 h.

To prepare lignin solutions, 0.5 and 1.5 g of low sulfonate lignin alkali powder were mixed with 9.5 g of formic acid in separate vials and stirred on a hot plate for 24 h at 100 °C. Then, the solutions were filtered using a 1.0 μm GD/X syringe filter. After that, 1.5 g of nylon 6 was added to each filtered solution, and they were left on a hot plate at 75 °C to homogenize completely.

Sericin solution was a blend of 1.5 g of silk sericin mixed with 9.5 g of formic acid under the same conditions as the zein solution described above. Then, 1.5 g of nylon 6 pellets were added to the solution, and the solution was left on the hot plate similarly to zein solutions.

To prepare the BSA solution, 10 wt % polyvinyl alcohol (PVA) solution in deionized water was prepared by stirring 1.0 g of PVA in 9.0 g of water for 4 h at 80 °C. Then, 1.0 g of BSA powder was added to the solution at room temperature and stirred for 10 min.

The 20 wt % PET solution was prepared by mixing 2.0 g of PET with 8 g of solution consisting of 30 wt % trifluoroacetic acid (TFA), 30 wt % dichloroacetic acid (DCA), and 40 wt % dichloromethane (DCM). The solution was kept at 55 °C on a hot plate for 4 h.

To produce soy protein/PET solution, 0.5 g of SP 781 was mixed with 2.0 g of dichloroacetic acid at high temperature (100 °C). SP solution was then added to 20 wt % solution of pure PET and left at 55 °C for 2 h to become completely homogeneous.

2.3. Solution Blowing and Sample Preparation. The solution-blowing setup was similar to the one used in the previous works of this group.[54,55] The setup is sketched in Figure 1, which describes it in brief.

To form monolithic nanofibers by solution blowing, a 13G stainless steel needle was placed coaxially inside an annular nozzle. Solution was pumped into the needle while air supplied from a high pressure line was issued through the annular nozzle using an upstream regulator. At the needle exit, the solution was exposed to a coaxial high-speed turbulent air jet. The

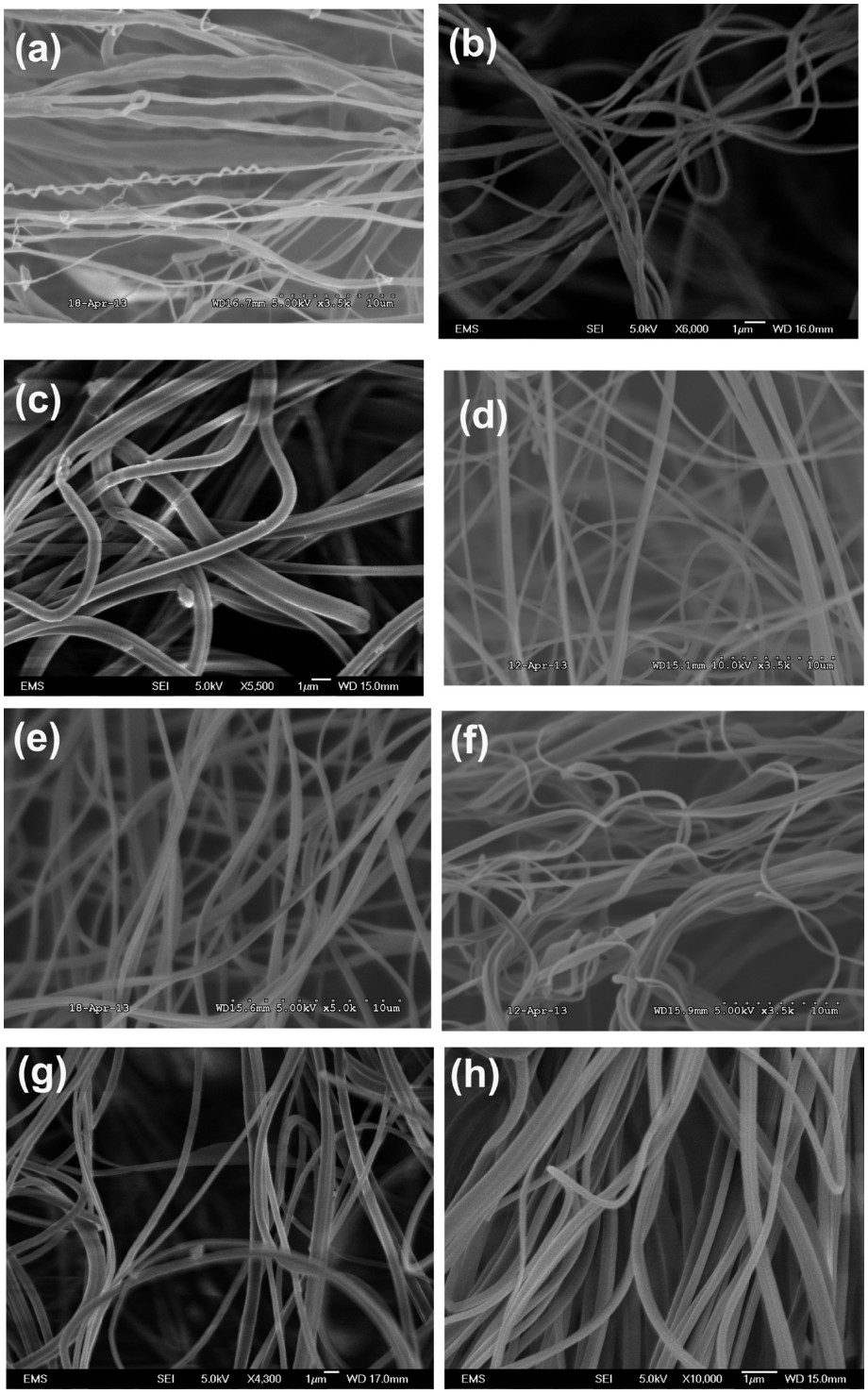

Figure 3. SEM micrographs of solution-blown nanofibers. Monolithic (a) BSA/PVA, (b) cellulose acetate/PAN, (c) lignin/nylon, (d) sericin/nylon, (e) sericin/zein/nylon, (f) soy protein/PET, (g) zein/nylon, and (h) core–shell zein/nylon nanofibers.

solution jet was stretched and bent due to the aerodynamic forces.[54,55] Core–shell nanofibers were formed as follows. An 18G stainless steel needle was located coaxially inside the 13G needle in the above-mentioned setup, and the outside coaxial nozzle was still used to issue air jet. Core solution was issued through the 18G needle, and the shell solution was issued from the 13G needle. For both monolithic and core–shell nanofiber blowing, the upstream pressure was kept constant at 2.0 bar, and solutions were issued at the rate of 4 mL/h. As a result, monolithic and core–shell nanofibers of 300–500 nm in diameter were formed.

Nanofibers were collected on a rotating drum covered with aluminum foil with a linear velocity at the circumference of about 2.9 m/s. The drum was placed 20 cm below the needle exit. As a result, collected nanofibers were partially oriented and prestretched in the winding direction. In each case, 5 mL of solution was issued from the needle to form the nanofiber mat. Collected nanofiber mats were removed from the foil as shown

dx.doi.org/10.1021/ie402246x | *Ind. Eng. Chem. Res.* 2013, 52, 15104–15113

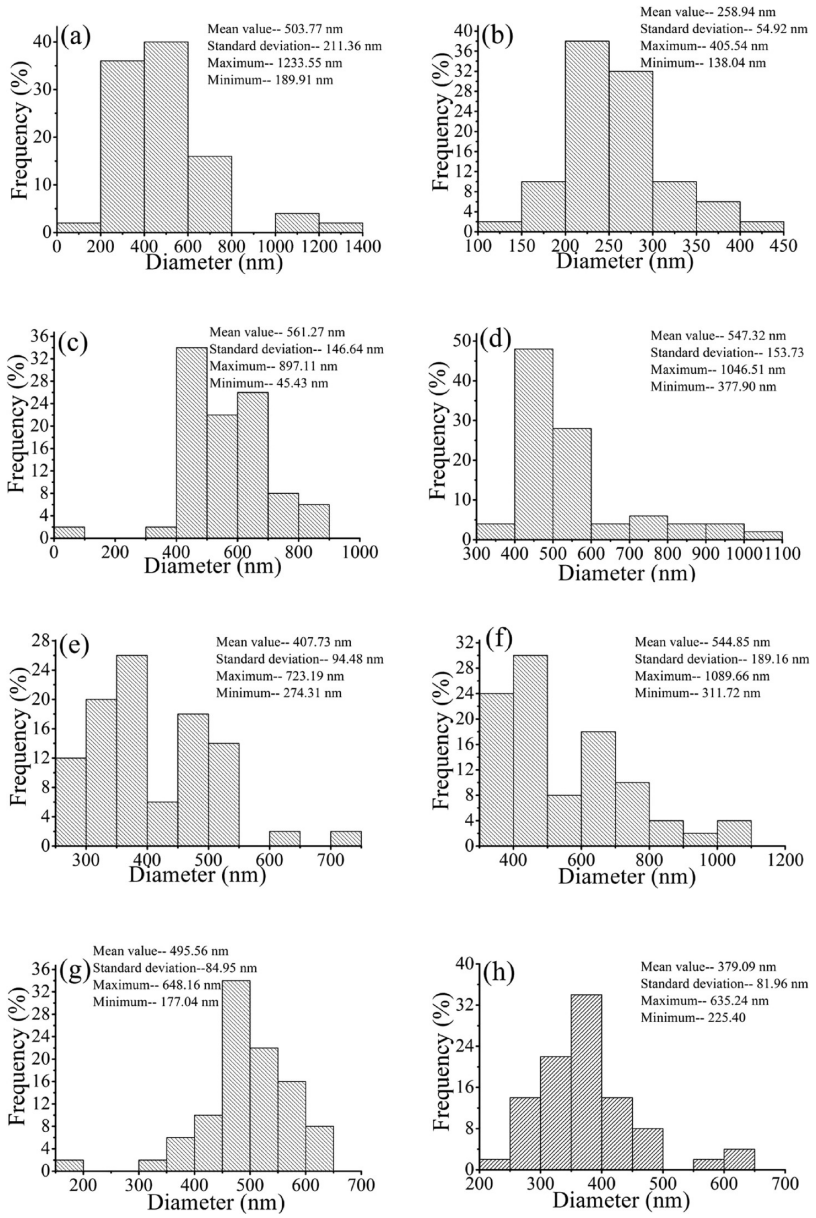

Figure 4. Fiber diameter distribution for (a) BSA/PVA (50:50) nanofibers, (b) cellulose acetate/PAN (50:50) nanofibers, (c) lignin/nylon 6 (50:50) nanofibers, (d) sericin/nylon 6(50:50) nanofibers, (e) sericin/zein/nylon 6 (25:25:50) nanofibers, (f) soy protein/PET (20:80) nanofibers, (g) zein/nylon 6 (57:43) nanofibers, and (h) core−shell zein/nylon 6 (70 wt % zein in the core) nanofibers. For each panel, the ensembles of more than 50 fibers were used.

in Figure 2 and cut into rectangular pieces with 5−10 mm width and 15−20 mm length. The thickness of these nanofiber mats was in the range 0.2−0.3 mm. Note that solution-blown BSA/PVA (50/50 wt %) nanofibers were collected on a solid substrate underneath the needle exit as randomly oriented nanofibers as shown in Figure 2.

Figure 2a shows monolithic cellulose acetate-based nanofiber mat with blended PAN as the host polymer. Monolithic soy protein/PET nanofibers are shown in Figure 2b. Currently, producing recyclable PET-containing materials is in focus in the literature. Therefore, the monolithic soy protein−PET nanofiber mats produced in this work is a significant step toward mass production of partially degradable PET-based nonwoven products. Figure 2c demonstrates monolithic nanofibers formed from a blend of two different biopolymers (soy protein and zein) and the host polymer nylon 6. Blending different biopolymers yields additional functionalities to such nonwovens. Similarly, combining biodegradable silk sericin and zein in a blend with nylon 6 is also possible (Figure 2g). Figure 2d depicts a monolithic zein/nylon 6 nanofiber mat, with more than 50 wt % zein content. Even at such a high content of biopolymer, the solution-blowing process was robust for a long time. The core−shell zein-based nanofiber mat is shown in Figure 2e. In this case, 70 wt % of core weight is zein. Core−shell nanofibers with high biopolymer content is a convenient way of enhancing the biodegradability of the material while sustaining mechanical and chemical durability comparable to those of purely synthetic products. Indeed, in such cases, biodegradable core material is protected by the synthetic shell. A monolithic lignin-based nanofiber mat with 50 wt % of biodegradable lignin is shown in Figure 2f. Monolithic fibers with 50 wt % of silk sericin formed by solution blowing are

dx.doi.org/10.1021/ie402246x | Ind. Eng. Chem. Res. 2013, 52, 15104−15113

Table 1. Average Mechanical Properties for Biopolymer-Containing Monolithic and Core−Shell Nanofiber Mats with Various Compositions and Contents[a]

sample	content (wt %)	solvent	ave. width (mm)	ave. thickness (mm)	ave. Young's modulus E (MPa)	ave. yield stress Y (MPa)	max. strain at rupture (%)	max. stress at rupture (MPa)
zein/nylon	40/60	formic acid	8.44	0.20	12.53 ± 2.55	0.16 ± 0.07	2.21 ± 0.76	0.19 ± 0.06
zein/nylon	57/43	formic acid	6.47	0.20	3.38 ± 1.69	0.10 ± 0.02	5.56 ± 1.44	0.13 ± 0.02
zein/nylon	66/34	formic acid	7.08	0.20	2.16 ± 0.74	0.04 ± 0.01	4.28 ± 0.92	0.06 ± 0.01
core−shell zein	Core: 70/30	formic acid	6.44	0.20	6.05 ± 0.69	0.30 ± 0.01	12.22 ± 0.62	0.47 ± 0.03
SP/zein/nylon	25/25/50	formic acid	6.93	0.20	10.90 ± 2.54	0.23 ± 0.04	5.63 ± 2.37	0.35 ± 0.06
zein/silk sericin/nylon	25/25/50	formic acid	6.50	0.15	20.46 ± 4.88	0.24 ± 0.05	2.50 ± 0.49	0.35 ± 0.06
silk sericin/nylon	50/50	formic acid	5.29	0.30	11.02 ± 2.16	0.22 ± 0.06	2.73 ± 0.41	0.28 ± 0.07
lignin/nylon	25/75	formic acid	5.53	0.16	23.39 ± 6.49	0.42 ± 0.08	4.13 ± 1.15	0.61 ± 0.10
lignin/nylon	50/50	formic acid	6.13	0.15	9.78 ± 2.41	0.22 ± 0.02	13.72 ± 3.76	0.38 ± 0.04
SP/PET	20/80	TFA/AC/DCM	6.55	0.20	28.59 ± 2.63	0.32 ± 0.11	0.88 ± 0.05	0.27 ± 0.04
cellulose AC/PAN	30/70	DMF	7.90	0.15	3.47 ± 2.67	0.23 ± 0.01	4.50 ± 1.17	0.15 ± 0.05
pure PET	100	TFA/AC/DCM	7.56	0.20	28.14 ± 3.24	0.37 ± 0.07	2.28 ± 0.31	0.50 ± 0.008

[a]SP stands for soy protein isolate.

shown in Figure 2h. In addition to the above-mentioned plant-derived biopolymers, monolithic nanofibers containing 50 wt % of an animal-derived protein BSA mixed with PVA were blown from an aqueous solution (Figure 2i). Because BSA's chemical structure and nanofiber architecture are similar to proteins and fibers in the human body, such systems hold great promise for tissue engineering and drug delivery. Note that the color of the nanofiber mat in Figure 2 is the true color under visible light. It is emphasized that Figure 2 demonstrates a wide variety of novel biodegradable nonwovens that can be formed by solution blowing at higher rates compared to other methods (e.g., electrospinning) of nanofiber forming.

2.4. Tensile Tests and Mechanical Characterization. Rectangular nanofiber mat samples underwent a uniaxial stretching test similar to our previous work.[57] The experiment was conducted using an Instron (model 5942) with cross-head speed of 1.0 mm/min at room temperature and humidity. The stretching continued until total failure of the samples. Stress−strain curves of the samples were measured, as were the maximum strain and stress at rupture ($\varepsilon_{rupture}$ and $\sigma_{xx,rupture}$, respectively). These features were used to characterize mechanical properties of biopolymer nanofibers using the phenomenological model discussed in ref 57. As a result, Young's modulus (E) and yield stress (Y) were found from the experimental stress−strain curves. It is emphasized that according to the SEM images of soy protein/nylon 6 nanofibers shown in ref 57, only 50% of the sample thickness is occupied with fibers, which implies that the applied stress is supported by only one-half of the samples' thickness, which was accounted for in data processing. For planar strips, stress−strain dependence in the elastic and plastic domain is described by the following equation[57]

$$\sigma_{xx} = \sqrt{\frac{8}{3}}\, Y \tanh\left(\sqrt{\frac{2}{3}}\,\frac{E}{Y}\varepsilon\right) \quad (1)$$

where σ_{xx} is tensile stress and ε is tensile strain.

2.5. Post-Processing of Solution-Blown Biopolymer Nanofiber Samples. In order to further improve the overall mechanical properties of biopolymer nanofibers, the samples underwent cold and hot drawing before some tensile tests. The samples were stretched up to 1% strain, with five equal intervals in between. The samples were kept at each intermediate strain for 5 min. This prestretching was conducted at room temperature (cold drawing), as well as at temperatures lower and higher than the polymer glass transition temperature of the host polymer. Drawing of macroscopic nylon and polyethylene fibers has been extensively discussed in ref 63. It was shown that the optimal drawing temperature is mostly close to the polymer glass transition temperature. In most cases, drawing increases crystallinity of polymer fibers as well as their strength.

2.6. Optical Observations. Morphology of biopolymer nanofibers was observed with a JEOL JSM-6320F scanning electron microscope under an 8 kV accelerating voltage. Samples were sputter-coated by platinum with 8 nm thickness before undergoing observation.

3. RESULTS AND DISCUSSION

3.1. Fiber Morphology and Fiber Size Distribution. SEM images of the solution-blown nanofiber mats are shown in Figure 3. Figures 3a−h show solution-blown monolithic BSA/PVA, cellulose acetate/PAN, lignin/nylon, sericin/nylon, sericin/zein/nylon, soy protein/PET, zein/nylon, and core−shell zein/nylon nanofibers, respectively. The resulting fiber size distribution found using the ensembles of more than 50 different fibers is shown in Figure 4. The fiber size distribution reveals that the average fiber diameter for BSA/PVA (50:50) fibers was 503.77 ± 211.36 nm. Similarly, for lignin/nylon 6 (50:50) fibers the average diameter was 561.27 ± 146.64 nm; for sericin/nylon 6 (50:50) fibers, 547.32 ± 153.73 nm; for soy protein/PET (20:80) nanofibers, 544.85 ± 189.16 nm; and for zein/nylon 6 (57:43) nanofibers, 495.56 ± 84.95 nm. Monolithic zein/sericin/nylon 6 (25:25:50) fibers revealed a lower value, with the diameter mean value of 407.73 ± 94.48 nm. The mean fiber diameter for core−shell zein-based nanofibers containing 70 wt % of zein in the core was 379.09 ± 81.96 nm. Solution blowing of cellulose acetate/PAN (50:50) nanofibers resulted in formation of fibers with the average diameter of 258.94 ± 54.92 nm, which is noticeably

dx.doi.org/10.1021/ie402246x | Ind. Eng. Chem. Res. 2013, 52, 15104−15113

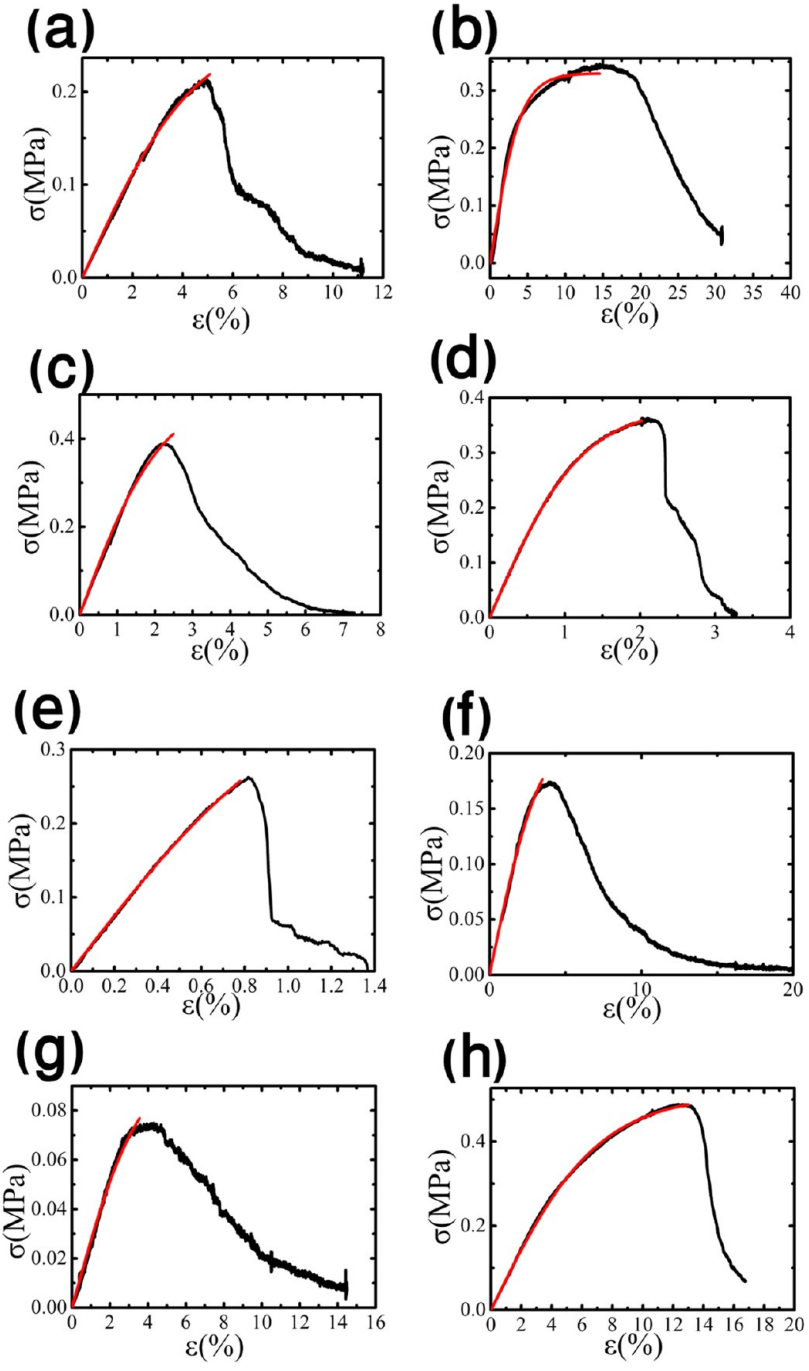

Figure 5. Stress−strain curves for plant-based protein solution-blown nanofiber mats for (a) monolithic cellulose acetate/PAN (30/70 wt %) nanofibers, (b) monolithic lignin/nylon 6 (50/50 wt %) nanofibers, (c) monolithic silk sericin/nylon 6 (50/50 wt %) nanofibers, (d) monolithic sericin/zein/nylon 6 (25/25/50 wt %) nanofibers, (e) monolithic soy protein/PET (20/80 wt %) nanofibers, (f) monolithic zein/nylon 6 (57/43 wt %) nanofibers, (g) monolithic zein/nylon 6 (66/34 wt %) nanofibers, and (h) core−shell zein/nylon 6 (70 wt % zein in core) nanofibers. Black curves show the experimental data, whereas red curves show their fit with eq 1.

lower than the average fiber diameter found for the other plant- and animal-based nanofibers.

Figures 2−4 show that solution blowing is capable of producing uniform nanofibers en masse from "agrowastes" and "animal proteins". The composition of all nanofibers formed is summarized in Table 1. It is emphasized that neither nanofibers nor macroscopic fibers with such a high content of biopolymers can be formed at a high rate by any other of the existing methods of fiber forming, as to our knowledge.

3.2. Mechanical Characterization of Biopolymer Nanofiber Samples. Table 1 summarizes the overall mechanical properties of different biopolymer-based nanofiber mats with various components and contents. The table includes data for both solution-blown monolithic and core−shell nanofiber samples that did not undergo any post-treatment. For each type of nanofiber mat, 30 rectangular samples were used in uniaxial tensile tests to obtain statistically confident results. The stress−strain curves measured for solution-blown protein-based nanofiber samples are shown in Figure 5.

Table 2. Overall Mechanical Properties of Soy Protein/PET (20/80 wt/wt %) Nanofiber Mats That Underwent Cold and Hot Drawing in Comparison to Non-Treated Samples

sample	average width (mm)	average thickness (mm)	average Young's modulus E (MPa)	average yield stress Y (MPa)	max. strain at rupture (%)	max. stress at rupture (MPa)
nontreated	6.55	0.20	28.59 ± 2.63	0.32 ± 0.11	0.88 ± 0.05	0.27 ± 0.04
cold drawn	6.47	0.20	28.96 ± 1.80	0.41 ± 0.09	0.83 ± 0.12	0.25 ± 0.06
hot drawn at 45 °C	6.77	0.20	30.42 ± 7.3	0.50 ± 0.29	0.88 ± 0.07	0.29 ± 0.04
hot drawn at 55 °C	5.5	0.20	44.57 ± 10.1	0.27 ± 0.04	0.29 ± 0.06	0.29 ± 0.06
hot drawn at 80 °C	5.71	0.20	64.05 ± 9.74	0.46 ± 0.16	0.518 ± 0.1	0.37 ± 0.05
hot drawn at 115 °C	5.26	0.20	55.98 ± 13.23	0.41 ± 0.13	0.28 ± 0.02	0.23 ± 0.06

Table 3. Average Mechanical Properties of Solution-Blown Nylon 6 Nanofiber Mats That Underwent Cold and Hot Drawing in Comparison to Non-Treated Samples

sample	average width (mm)	average thickness (mm)	average Young's modulus E (MPa)	average yield stress Y (MPa)	max. strain at rupture (%)	max. stress at rupture (MPa)
nontreated	9.53	0.20	15.06 ± 2.68	1.4 ± 0.06	14.24 ± 2.27	1.45 ± 0.03
cold drawn	7.66	0.20	19.091 ± 1.51	1.38 ± 0.09	12.0 ± 2.04	1.28 ± 0.06
hot drawn at 45 °C	7.71	0.20	18.42 ± 5.22	1.27 ± 0.06	11.48 ± 2.33	1.34 ± 0.08
hot drawn at 55 °C	7.52	0.20	18.97 ± 3.43	1.37 ± 0.10	12.91 ± 2.04	1.45 ± 0.11
hot drawn at 80 °C	6.92	0.20	15.77 ± 2.58	1.25 ± 0.04	13.03 ± 1.85	1.25 ± 0.05
hot drawn at 115 °C	7.39	0.20	22.65 ± 3.45	1.40 ± 0.10	10.57 ± 1.81	1.50 ± 0.18

The average Young's modulus of soy protein/nylon 6 (40/60 wt/wt %) monolithic nanofiber samples measured using tensile tests was reported in ref 57 as 19.56 ± 6.48 MPa. The monolithic zein/nylon 6 nanofiber samples (40/60 wt/wt %) revealed a lower value of Young's modulus. As reported in Table 1, Young's modulus of zein/nylon 6 (40/60 wt/wt %) samples is 12.53 ± 2.55 MPa. As zein content increased and nylon 6 content decreased correspondingly in the nanofiber samples, Young's modulus and the average yield stress decreased. For samples with 66 wt % of zein, Young's modulus was almost five times lower than the one for the samples with 40 wt % of zein. The average yield stress of zein-containing samples follows the same trend: a four time decrease occurred in the yield stress for 66 wt % zein-containing samples compared to the samples that contained 40 wt % of zein. However, the core−shell zein-based nanofibers follow a different trend than the monolithic ones. Although core−shell zein/nylon 6 nanofiber mats contained a higher amount of zein (i.e., 70 wt %), their Young's modulus was found to be higher than that of the monolithic nanofibers containing almost the same amount of zein. The core−shell structure with zein in the core is definitely beneficial because monolithic zein nanofibers are generally weaker than, for example, soy-protein-containing ones.

For those monolithic nanofibers that were comprised of both zein and soy protein, the average Young's modulus was found to be higher than that of the zein-containing nanofibers and lower than the one reported in ref 58 as an average value of Young's modulus for soy protein-nylon 6 (50/50 wt %) nanofiber mats.

Lignin nanofibers revealed lower Young's modulus compared to those of comparable soy protein-containing samples as reported in ref 58, yet the strength of lignin/nylon 6 (50/50 wt %) samples is slightly higher than zein-containing samples with almost the same content percentage. Higher nylon 6 content in the lignin nanofiber mats [lignin/nylon 6 (25/75 wt/wt %)] led to stronger samples, with an average Young's modulus of 23.39 ± 6.49 MPa.

Silk protein/nylon 6 (50/50 wt %) samples revealed the average strength close to that of lignin-containing nanofiber mats with the same content.

Solution-blown soy protein/PET nanofiber mats revealed a higher Young's modulus compared to the one for solution-blown pure nylon 6 nanofiber samples studied in ref 57. For control, pure PET nanofibers were also produced using solution blowing and collected similarly to the biopolymer-based samples. Pure PET nanofiber mats had an average Young's modulus of 28.14 ± 3.24 MPa, which is close to the modulus of soy protein/PET (20/80 wt %) mats, which was 28.59 ± 2.63 MPa. Due to the wide range of the industrial applications of PET-based products, it is desirable to develop partially biodegradable PET samples where sustaining their mechanical properties is not compromised, as is achieved in the present work.

Monolithic cellulose acetate/PAN samples showed lower Young's modulus compared to the other biopolymer samples with nylon 6 or PET as a synthetic part of the nanofibers.

3.3. Cold and Hot Drawing of Nanofiber Mats. The effect of physical cross-linking on nylon-based soy protein nanofibers was discussed in ref 58. In some nanofibers in the present work, nylon is used as the host polymer. Therefore, qualitatively, the relative effect of physical cross-linking on such fibers is expected to be similar to that in ref 58. In addition, in the present work, PET was also used as a host polymer. The effect of drawing on soy protein/PET (20/80 wt/wt %) nanofibers is reported in Table 2. All these samples were prestretched up to 1% strain, with five equal intervals in between. Drawing of soy protein/PET nanofiber samples was

dx.doi.org/10.1021/ie402246x | Ind. Eng. Chem. Res. 2013, 52, 15104−15113

conducted at 45, 55, 80, and 115 °C (hot drawing). Maximum increase in samples' Young's modulus was observed at 80 °C: the average Young's modulus was almost doubled compared to that of the nontreated samples. Nontreated soy protein/PET nanofiber mats revealed average Young's modulus of 28.59 ± 2.63 MPa. The average Young' modulus increased to 64.05 ± 9.74 MPa for samples post-treated at 80 °C. Note that glass transition temperature for PET is in the range 76−81 °C. In ref 58, physical post-treatment of soy protein/nylon solution-blown nanofiber mats was investigated, and thermal and wet bonding procedures were separately examined on soy protein/nylon nanofibers. Specifically, thermal bonding of nylon-based nanofibers led to a 50% increase in the average Young's modulus of the samples. Wet bonding resulted in about a 65% increase in the samples' Young's modulus. Therefore, hot drawing of nanofiber samples around the host polymer's glass transition temperature significantly affected the sample strength because an almost 100% increase in samples' Young's modulus was observed. For comparison, Table 3 elucidates the effect of cold and hot drawing on pure solution-blown nylon 6 nanofiber samples. Note that glass transition temperature for nylon 6 is 47 °C, yet the drawing post-treatment did not affect the samples' mechanical properties significantly. The mean Young's modulus value for nontreated pure nylon 6 solution-blown nanofibers was found as 15.06 ± 2.68 MPa. Samples which underwent hot drawing close to nylon's glass transition temperature (i.e., hot drawing at 45 °C) did not reveal a significant increase in their average Young's modulus. Hot drawn samples at 45 °C showed average Young's modulus of 18.42 ± 5.22 MPa

4. CONCLUSION

Solution blowing was successfully applied to form nanofiber mats comprised of different plant- and animal-derived proteins. Soy protein, cellulose acetate, zein, silk sericin, lignin, and different blends of these materials were used to produce monolithic and core−shell plant-protein-derived nanofibers. These biopolymers were mixed with such synthetic polymers as nylon 6 and PET to enhance their overall mechanical properties. Bovine serum albumin (an animal-derived protein) also underwent solution blowing and was used to form BSA/PVA (50/50 wt %) nanofibers, which are of interest for wound dressing, as drug carriers, and for other applications due to their biocompatibility and biodegradability. Solution blowing of pure synthetics polymers was also demonstrated in the present work by producing PET nanofibers. Their tensile strength was also measured for control. All of the above-mentioned nanofibers were collected as nonwoven mats, and their Young's modulus and yield stress were estimated using the phenomenological Prager equation. Forming nanofibers from plant- and animal-derived proteins using solution blowing holds great promise for their industrial application because these biocompatible and biodegradable nanofibers can be produced at rates incomparably higher than those of electrospinning.

AUTHOR INFORMATION

Corresponding Author

*A. L. Yarin. Phone: +1-312 996 3472. Fax: +1-312 413-0447. E-mail: ayarin@uic.edu.

Notes

The authors declare no competing financial interest.

ACKNOWLEDGMENTS

This work was partially supported by the United Soybean Board, Chesterfield, Missouri.

REFERENCES

(1) Mahonty, A. K.; Misra, M.; Hinrichsen, G. Biofibres, biodegradable polymers and biocomposites: An overview. *Macromol. Mater. Eng.* **2000**, *276/277*, 1−24.
(2) Andrady, A. L. Biodegradability of Polymers. In *Physical properties of polymers handbook*; Mark, J. E., Ed.; Springer: New York, 2007, 951−964.
(3) Kint, D.; Munoz-Guerra, S. A review on the potential biodegradability of poly(ethylene terephthalate). *Polym. Int.* **1999**, *48*, 346−352.
(4) Wellen, R.; Canedo, E.; Rabello, M. Effect of styrene-co-acrylonitrile on cold crystallization and mechanical properties of poly(ethylene terephthalate). *J. Appl. Polym. Sci.* **2012**, *125*, 2701−2710.
(5) Huang, J.; Zhang, L.; Chen, F. Effects of lignin as a filler on properties of soy protein plastics. I. lignosulfonate. *J. Appl. Polym. Sci.* **2003**, *88*, 3284−3290.
(6) Chandra, R.; Rustgi, R. Biodegradable Polymers. *Prog. Polym. Sci.* **1998**, *23*, 1273−1335.
(7) Kaplan, D. L. *Biopolymers from renewable resources*; Springer: Berlin, 1998.
(8) Liu, K. S. *Soybeans: chemistry, technology, and utilization*; Chapman & Hall: New York, 1997.
(9) Paetau, I.; Chen, C. Z.; Jane, J. L. Biodegradable plastic made from soybean products. 1. Effect of preparation and processing on mechanical properties and water. *Ind. Eng. Chem. Res.* **1994**, *33*, 1821−1827.
(10) Sue, H. J.; Wang, S.; Jane, J. L. Morphology and mechanical behavior of engineering soy plastics. *Polym. J.* **1997**, *38*, 5035−5040.
(11) Mo, X.; Sun, X. S.; Wang, Y. Effects of molding temperature and pressure on properties of soy protein polymers. *J. Appl. Polym. Sci.* **1999**, *73*, 2595−2602.
(12) Zhang, J.; Mungara, P.; Jane, J. Mechanical and thermal properties of extruded soy protein sheets. *Polym. J.* **2001**, *42*, 2569−2578.
(13) O'Sullivan, A. C. Cellulose: the structure slowly unravels. *Cellulose* **1997**, *4*, 173−207.
(14) Stephen, A. M. *Food polysaccharides and their applications*; CRC Press: Boca Raton, FL, 2006.
(15) Kamide, K. *Cellulose and cellulose derivatives*; Elsevier B.V.: Amsterdam, 2005.
(16) Krassig, H. *Cellulose: Structure, accessibility and reactivity*; CRC Press: Boca Raton, FL, 1993.
(17) Gemili, S.; Yeminicioglu, A.; Altinkaya, S. A. Development of cellulose acetate based antimicrobial food packaging materials for controlled release of lysozyme. *J. Food Eng.* **2009**, *90*, 453−462.
(18) Roman, M.; Dong, S. P.; Hirani, A.; Lee, Y. W. Cellulose nanocrystals for drug delivery. In *Polysaccharide Materials: Performance by Design*; Edgar, K., Ed.; ACS Symposium Series 1017; American Chemical Society: Washington, DC, 2010; 81−91.
(19) Carroll, A.; Somerville, C. Cellulosic Biofuels. *Annu. Rev. Plant Biol.* **2009**, *60*, 165−182.
(20) Coyle, W.*The future of biofuels- A global perspective*; Amber Waves, USDA, ERS: Washington, DC, 2007.
(21) Giampietro, M.; Ulgiati, S.; Pimentel, D. Feasibility of large-scale biofuel production. *BioScience* **1997**, *47*, 587−600.
(22) Ma, Z.; Kotaki, M.; Ramakrishna, S. Electrospun cellulose nanofiber as affinity membrane. *J. Membr. Sci.* **2005**, *265*, 115−123.
(23) Chen, G.; Liu, H. Electrospun cellulose nanofiber reinforced soybean protein isolate composite film. *J. Appl. Polym. Sci.* **2008**, *110*, 641−646.
(24) Zhou, W.; He, J.; Du, S.; Cui, S.; Gao, W. Electrospun silk fibroin/cellulose acetate blend nanofibres: structure and properties. *Iran. Polym. J.* **2011**, *20*, 389−397.

(25) Peng, B. L.; Dhar, N.; Liu, H. L.; Tam, K. C. Chemistry and applications of nanocrystalline cellulose and its derivatives: a nanotechnology perspective. *Can. J. Chem. Eng.* **2011**, *9999*, 1−16.
(26) Han, S. O.; Youk, J. H.; Min, K. D.; Kang, Y. O.; Park, W. H. Electrospining of cellulose acetate nanofibers using a mixed solvent of acetic acid/water: Effects of solvent composition on the fiber diameter. *Mater. Lett.* **2008**, *62*, 759−762.
(27) Son, W. K.; Youk, J. H.; Lee, T. S.; Park, W. H. Electrospinning of ultrafine cellulose acetate fibers: studies of a new solvent system and deacetylation of ultrafine cellulose acetate fibers. *J. Polym. Sci., Part B: Polym. Phys.* **2004**, *42*, 5−11.
(28) Zhou, W.; He, J.; Cui, S.; Gao, W. Studies of Electrospun cellulose acetate nanofibrous membranes. *Open Mater. Sci. J.* **2011**, *5*, 51−55.
(29) Liu, H.; Hsieh, Y. L. Ultrafine fibrous cellulose membranes from electrospinning of cellulose acetate. *J. Polym. Sci., Part B: Polym. Phys.* **2002**, *40*, 2119−2129.
(30) Frey, M. W. Electrospinning cellulose and cellulose derivatives. *Polym. Rev.* **2008**, *48*, 378−391.
(31) Vanholme, R.; Demedts, K.; Ralph, J.; Boerjan, W. Lignin biosynthesis and structure. *Plant Physiol.* **2010**, *153*, 895−905.
(32) Bhatnagar, A.; Sain, M. Processing of cellulose nanofiber-reinforced composites. *J. Reinf. Plast. Compos.* **2005**, *24*, 1259−1268.
(33) Kadla, J. F.; Kubo, S.; Venditti, R. A.; Gilbert, R. D.; Compere, A. L.; Griffith, W. Lignin-based carbon fibers for composite fiber applications. *Carbon* **2002**, *40*, 2913−2920.
(34) Seo, D. K.; Jeun, J. P.; Kim, H. B.; Kang, P. H. Preparation and characterization of the carbon nanofiber mat produced from electrospun PAN/lignin precursors by electron beam irradiation. *Rev. Adv. Mater. Sci.* **2011**, *28*, 31−34.
(35) Braun, J. L.; Holtman, K. M.; Kadla, J. F. Lignin-based carbon fibers: Oxidative thermostabilization of kraft lignin. *Carbon* **2005**, *43*, 385−394.
(36) Liu, T.; Gu, S. Y.; Zhang, Y. H.; Ren, J. Fabrication and characterization of carbon nanofibers with a multiple tubular porous structure via electrospinning. *J. Polym. Res.* **2012**, *19:9882*, 1−6.
(37) Kim, C.; Jeong, Y.; Ngoc, B. T. N.; Yang, K. S.; kojima, M.; Kim, Y. A.; Endo, M.; Lee, A. Y. Synthesis and characterization of porous carbon nanofibers with hollow cores through the thermal treatment of electrospun copolymeric nanofiber webs. *Small: Nano Micro.* **2007**, *3*, 91−95.
(38) Shukla, R.; Cheryan, M. Zein: the industrial protein from corn. *Ind. Crop. Prod.* **2001**, *13*, 171−192.
(39) Gianazza, E.; Viglienghi, V.; Righetti, P. G.; Salamini, F.; Soave, C. Amino acid composition of zein molecular components. *Phytochemicals* **1977**, *16*, 315−317.
(40) Geraghty, D.; Peifer, M. A.; Rubenstein, I.; Messing, J. The primary structure of a plant storage protein: zein. *Nucleic Acid Res.* **1981**, *9*, 5163−5174.
(41) Kanjanapongkul, K.; Wongsasulak, S.; Yoovidhya, T. Prediction of clogging time during electrospinning of zein solution: Scaling analysis and experimental verification. *Chem. Eng. Sci.* **2010**, *65*, 5217−5225.
(42) Yao, C.; Li, X.; Song, T. Electrospinning and crosslinking of zein nanofiber mats. *J. Appl. Polym. Sci.* **2006**, *103*, 380−385.
(43) Miyoshi, T.; Toyohara, K.; Minematsu, H. Preparation of ultrafine fibrous zein membranes via electrospinning. *Polym. Int.* **2005**, *54*, 1187−1190.
(44) Padamwar, M. N.; Pawar, A. P. Silk sericin and its applications: a review. *J. Sci. Ind. Res.* **2004**, *63*, 323−329.
(45) Zhang, H.; Magoshi, J.; Magoshi, Y.; Yoshida, H.; Chen, J. Y.; Saiki, K. Inorganic composition and thermal properties of cocoon fiber. *Int. J. Soc. Mater. Eng. Resour.* **2002**, *10*, 113−116.
(46) Jin, H. J.; Fridrikh, S. V.; Rutledge, G. C.; Kaplan, D. L. Electrospinning Bombyx mori silk with poly(ethylene oxide). *Biomacromolecules* **2002**, *3*, 1233−1239.
(47) Li, C.; Vepari, C.; Jin, H. J.; Kim, H. J.; Kaplan, D. L. Electrospun silk-BMP-2 scaffolds for bone tissue engineering. *Biomaterials* **2006**, *27*, 3115−3124.
(48) Zhang, Y. Q. Applications of natural silk protein sericin in biomaterials. *Biotechnol. Adv.* **2002**, *20*, 91−100.
(49) Peters, T. Jr. *All About Albumin: Biochemistry, Genetics, and Medical Applications*; Academic Press: Salt Lake City, UT, 1996.
(50) Curry, S.; Brick, P.; Franks, N. P. Fatty acid binding to human serum albumin: new insights from crystallographic studies. *Biochim. Biophys. Acta* **1999**, *1441*, 131−140.
(51) Liao, I.; Chew, S. Y.; Leong, K. W. Aligned cores-shell nanofibers delivering bioactive proteins. *Nanomedicine* **2006**, *1*, 465−471.
(52) Dror, Y.; Ziv, T.; Makarov, V.; Wolf, H.; Admon, A.; Zussman, E. Nanofibers made of globular proteins. *Biomacromolecules* **2008**, *9*, 2749−2754.
(53) Valmikinathan, C. M.; Defroda, S.; Yu, X. Polycaprolactone and bovine serum albumin based nanofibers for controlled release of nerve growth factor. *Biomacromolecules* **2009**, *10*, 1084−1089.
(54) Sinha-Ray, S.; Yarin, A. L.; Pourdeyhimi, B. The production of 100/400 nm inner/outer diameter carbon tubes by solution blowing and carbonization of core−shell nanofibers. *Carbon* **2010**, *48*, 3575−3578.
(55) Sinha-Ray, S.; Zhang, Y.; Yarin, A. L.; Davis, S.; Pourdeyhimi, B. Solution blowing of soy protein fibers. *Biomacromolecules* **2011**, *12*, 2357−2363.
(56) Zhuang, X.; Yang, X.; Shi, L.; Cheng, B.; Guan, K.; Kang, W. Solution blowing of submicron-scale cellulose fiber. *Carbohydr. Polym.* **2012**, *90*, 982−987.
(57) Khansari, S.; Sinha-Ray, S.; Yarin, A. L.; Pourdeyhimi, B. Stress-strain dependence for soy-protein nanofiber mats. *J. Appl. Phys.* **2012**, *111*, 044906−1−13.
(58) Sinha-Ray, S.; Khansari, S.; Yarin, A. L.; Pourdeyhimi., B. Effect of chemical and physical cross-linking on tensile characteristics of solution-blown soy protein nanofiber mats. *Ind. Eng. Chem. Res.* **2012**, *51*, 15109−15121.
(59) Karck, M.; Forgione, L.; Haverich, A. The efficacy of controlled antibiotic release: for prevention of polyethyleneterephthalate-(Dacron) related infection in cardiovascular surgery. *Clin. Mater.* **1993**, *13*, 149−154.
(60) Dewanjee, M. K.; Gross, D. R.; Zhai, P.; Lanzo, S.; Shim, H.; Park, K.; Schaeffer, D. J.; Twardock, A. R. Thrombogenicity of polyethylene oxide-bonded Dacron sewing ring in a mechanical heart valve. *J. Heart Valve Disease* **1999**, *8*, 324−330.
(61) Smith, T. P.; Alexander, M. J.; Enterline, D. S. Delayed stenosis following placement of a polyethylene terephthalate endograft in the cervical carotid artery. Report of three cases. *J. Neurosurg.* **2003**, *98*, 421−425.
(62) Wang, J.; Huang, N.; Yang, P.; Leng, Y. X.; Sun, H.; Liu, Z. Y.; Chu, P. K. The effects of amorphous carbon films deposited on polyethylene terephthalate on bacterial adhesion. *Biomaterials* **2004**, *25*, 3163−3170.
(63) Ziabicki, A. *Fundamentals of fiber formation: The science of fiber spinning and drawing*; Wiley: London, 1976.